from the effect of the electrostriction. Hence, $\Delta V_1°$ values is estimated to be about 5.6 cm^3 mol^{-1} for the present systems.

Volume profiles for the complexation reactions of nickel(II) glycolate and nickel(II) lactate are shown in Figure 3 where $\Delta V_{os}°$ and $\Delta V_1°$ were derived as described above. As is seen from this figure, almost similar features were obtained for both systems; the difference in the structures of glycolic acid and lactic acid is only the methyl group on the α-carbon. The volume change associated with chelation by the hydroxyl group is estimated to be about 9 cm^3 mol^{-1}, which is larger than $\Delta V_1°$ by about 3 cm^3 mol^{-1}. This difference in the volume change may be ascribed partly to the fact that the interaction between nickel(II) and the hydroxyl oxygen is weak and the bond length is longer than that between nickel(II) and the carboxyl oxygen and partly to the increase in free volume accompanied by the formation of ring structure, which is too small to be occupied by the solvent molecule.[1] At the present time, these two contributions can not be estimated separately. If the latter contribution is neglected tentatively, it is shown by the calculation using the van der Waals radii of oxygen that the difference in the volume change by 3 cm^3 mol^{-1} corresponds to the difference in the bond length by about 0.8 Å.

The activated state of the overall complexation reaction is in the course of the chelation process and may be considered to be the state where the bond between nickel(II) and the hydroxyl oxygen is partly formed. The positive activation volume may be attributed to the two factors: (i) The bond length between nickel(II) and the hydroxyl oxygen at an activated state is longer than that between the metal and water at an initial state (III) (i.e., "structural" term). (ii) The hydrated water around the hydroxyl group is partly eliminated to form the free water in order to attain the activated state (i.e., "solvation" term). It is impossible to separate the present ΔV_2^* into the two terms. However, it may be considered qualitatively that the contribution from the solvation term is more significant for the chelation process, because, if otherwise, the formation of the final stable chelate (IV) from the activated state should accompany the negative volume change. A slight difference in ΔV_2^* for nickel(II) glycolate and nickel(II) lactate might be regarded as reflecting the difference in the bond length between nickel(II) and the hydroxyl oxygen at an activated state, which may be reflected to ΔV_2^* through the bond length itself and the degree of desolvation. However, more detailed discussion on this report is not given at the present time.

Acknowledgment. This work was supported financially in part by the Central Research Institute of Fukuoka University.

Registry No. Nickel, 7440-02-0; glycolic acid, 79-14-1; lactic acid, 50-21-5.

Contribution from the Department of Inorganic Chemistry, The Royal Institute of Technology, S-100 44 Stockholm, Sweden

Studies of Metal Carbonate Equilibria. 8. Structure of the Hexakis(carbonato)tris[dioxouranate(VI)] Ion in Aqueous Solution. An X-ray Diffraction and ^{13}C NMR Study

MÄRTHA ÅBERG,* DIEGO FERRI, JULIUS GLASER, and INGMAR GRENTHE

Received February 28, 1983

The X-ray scattering from moderately concentrated dioxouranium(VI) carbonate solutions with the major part of uranium bound in the trinuclear complex $(UO_2)_3(CO_3)_6^{6-}$ has been measured. A model for the structure of this complex consistent with the scattering data and compatible with ^{13}C NMR data is suggested. The complex is triangular with a U–U distance of 4.946 (5) Å. There are two sets of coordinated carbonate ions, three bridging and three terminal ones. The latter are bonded through two oxygens to uranium. The bridges are formed through bidentate coordination of the carbonate ion to two uranium atoms. The overall symmetry of the complex is close to D_{3h}, and each uranium(VI) has an approximately hexagonal-bipyramidal coordination geometry, similar to those found in e.g. $UO_2CO_3(s)$ and $K_4[UO_2(CO_3)_3](s)$. The ^{13}C NMR chemical shifts for the two types of carbonate ions in the complex have been determined to be 168.7 and 167.3 ppm, respectively, from Me_4Si.

Introduction

The equilibria between UO_2^{2+}, H_2O, and $CO_2(g)$ at 25 °C in a 3 M $NaClO_4$ medium have been studied at acidities ranging from $[H^+] \simeq 10^{-5}$ M to $[H^+] \simeq 10^{-7}$ M by potentiometric measurements.[1] The data could be explained by assuming the equilibrium

$$3UO_2(CO_3)_3^{4-} + 6H^+ \rightleftharpoons (UO_2)_3(CO_3)_6^{6-} + 3CO_2(g) + 3H_2O$$

The structure of the mononuclear complex $UO_2(CO_3)_3^{4-}$ is well-known from crystal structures.[2-4] There is no reason to believe that the structure in solution is very much different.

The structure of the trinuclear complex $(UO_2)_3(CO_3)_6^{6-}$ is unknown. Preliminary ^{13}C NMR data[1] have indicated the presence of two types of coordinated carbonate ions, presumably bridging and terminal ones.

Fairly concentrated solutions, where more than 80% of the total uranium is bound in the trinuclear complex, can be prepared. Hence, it seems likely that X-ray investigations can give information on the structure of the complex in solution.

Experimental Section

Materials and Analysis. Dioxouranium(VI) (uranyl) perchlorate solutions, perchloric acid, sodium hydrogen carbonate, and sodium perchlorate were prepared and analyzed as described elsewhere.[1]

Uranyl nitrate solutions were prepared from $UO_2(NO_3)_2(H_2O)_6$ (Merck, reagent grade) without further purification. They were

(1) Ciavatta, L.; Ferri, D.; Grenthe, I.; Salvatore, F. *Inorg. Chem.* **1981**, *20*, 463.
(2) Graziani, R.; Bombieri, G.; Forsellini, E. *J. Chem. Soc., Dalton Trans.* **1972**, 2059.
(3) Anderson, A.; Chieh, C.; Irish, D. E.; Tong, J. P. K. *Can. J. Chem.* **1980**, *58*, 1651.
(4) Coda, A.; Della Giusta, A.; Tazzoli, V. *Acta Crystallogr., Sect. B* **1981**, *B37*, 1496.

0020-1669/83/1322-3981$01.50/0

Table I. Compositions of the Solutions Investigated by X-ray Diffraction[a]

	solution		
	B1	B2	C
Z	4.22	4.11	4.3
α	0.892	0.942	0.83
V, Å^3	3327.7	2767.3	1845
d, g cm^{-3}	1.250	1.306	1.41
$[UO_2^{2+}]$, M	0.499	0.600	0.9
$[ClO_4^-]$, M	1.000	1.220	
$[NO_3^-]$, M			1.8
$[CO_3^{2-}] + [HCO_3^-]$, M	1.055	1.246	1.95
$[Na^+]$, M	2.110	2.500	3.9
$[H_2O]$, M	50.18	49.42	47.1

[a] Z = average number of OH groups per U atom in $(UO_2)_p(OH)_q(CO_2)_r$ as calculated from the partial pressure of CO_2(g) and the hydrogen ion concentration of the solution ($(OH)_2CO_2^{2-} \equiv CO_3^{2-}$). α = fraction of total uranium bound in $(UO_2)_3(CO_3)_6^{6-}$. V = volume of a stoichiometric unit of solution containing one U atom. d = density of the solution.

analyzed according to the procedure described for the perchlorate solutions.[1]

The compositions of the solutions investigated by X-ray diffraction are given in Table I.

Solutions investigated by ^{13}C NMR were as a rule prepared by using ^{13}C-enriched (90%) $NaHCO_3$ of reagent grade.

NMR Measurements. Carbon-13 NMR spectra were recorded at 50.3 MHz (Bruker WP200 spectrometer) by using spinning 10-mm tubes. Internal D_2O (10%) was used as the field lock. The chemical shifts are given in ppm toward higher frequency with respect to tetramethylsilane (Me_4Si). An external methanol reference was taken as 49.3 ppm from Me_4Si.

X-ray-Scattering Measurements. The diffractometer was the same as described previously.[5] Ag K radiation ($\lambda_{K\alpha} = 0.5608$ Å) was used in order to minimize the fluorescent radiation.[6] In a preliminary investigation, which was not carried out with the highest accuracy possible, solution C was studied by using Mo K radiation ($\lambda_{K\alpha} = 0.7107$ Å). A precipitate was formed toward the end of the measuring period. For the other two solutions, the scattering measurements were made in the usual way.[7] CO_2(g) was passed over the solutions in order to keep the hydrogen ion concentration constant. The intensity data were corrected for background and for absorption[8] before they were recalculated to a common slit width.

Symbols

V	stoichiometric unit of volume
Z	average number of OH groups per U atom, where $(OH)_2CO_2^{2-} \equiv CO_3^{2-}$
del(s)	fraction of the total incoherent scattering passing through the monochromator
2θ	scattering angle
s	$4\pi\lambda^{-1} \sin\theta$
$i(s)$	reduced intensity values
$I(s)$	normalized intensity values after corrections for background, absorption, polarization, multiple scattering, and fluorescent radiation
n_i	number of atoms i per unit volume
$I_i^{incoh}(s)$	incoherent scattering of atom i
$f_i(s)$	scattering factor for atom i
$\Delta f_i'$	real part of the anomalous dispersion correction for atom i
$\Delta f_i''$	imaginary part of the anomalous dispersion correction for atom i
$D(r)$	electronic radial distribution function
ρ_0	average scattering density per unit volume
$M(s)$	modification function for the Fourier inversions
$i_{pq}(s)$	pair interaction function for the atom pair pq
n_j	number of complexes j per unit volume
r_{pq}	distance between atoms p and q
l_{pq}	root-mean-square variation of the distance between atoms p and q
b_{pq}	$l_{pq}^2/2$
n_{pq}	number of interactions for the atom pair pq
U	error-square sum used in PUTSLR[9]
$w(s)$	weighting function used in PUTSLR[9]

Treatment of the Intensity Data. All calculations were carried out with use of the KURVLR and PUTSLR programs.[9]

The measured intensity data were corrected for polarization and multiple scattering.[9] The del(s) function was estimated as described previously.[5] Corrections for fluorescent radiation were made in an empirical way.[6]

The reduced intensity values, $i(s)$, were calculated according to the expression

$$i(s) = I(s) - [\mathrm{del}(s)]\sum_i n_i[I_i^{incoh}(s)] - \sum_i n_i\{[f_i(s) + \Delta f_i']^2 + (\Delta f_i'')^2\}$$

They were corrected for low-frequency errors, resulting in spurious peaks below 1 Å in the radial distribution curves that could not correspond to interatomic distances.[9]

From the $i(s)$ values, the electronic radial distribution functions were calculated as

$$D(r) = 4\pi r^2\rho_0 + 2r/\pi \int_0^{s_{max}} s[i(s)][M(s)] \sin(rs)\, ds$$

The modification function was

$$M(s) = \{[f_U(0) + \Delta f_U']^2 + (\Delta f_U'')^2\}/\{[f_U(s) + \Delta f_U']^2 + (\Delta f_U'')^2\} \exp(-0.01s^2)$$

Theoretical pair interaction functions were calculated according to the expression

$$i_{pq}(s) = 2\sum_j n_j \sum_{p \neq q} \sum_{p \neq q} \sum_q \{[f_p(s) + \Delta f_p'][f_q(s) + \Delta f_q'] + \Delta f_p''\, \Delta f_q''\}[\sin(r_{pq}s)](r_{pq}s)^{-1} \exp(-b_{pq}s^2)$$

The Fourier inversion of $\sum i_{pq}$ was made in the same way as that of the experimental values.

The scattering factors, $f_i(s)$, were taken from Cromer and Waber.[10] For H, however, the values given by Stewart et al.[11] were chosen, and for H_2O, the molecular scattering factors given by Narten and Levy[12] were used. Anomalous dispersion corrections, $\Delta f_i'$ and $\Delta f_i''$, were those given by Cromer.[13] Values for the incoherent scattering were taken from Cromer for all atoms except H.[14] For H, Compton and Allison's data were used.[15] Corrections for the Breit–Dirac factor were applied.

Results and Discussion

^{13}C NMR. Solutions containing known amounts of $(UO_2)_3(CO_3)_6^{6-}$, $UO_2(CO_3)_3^{4-}$, and HCO_3^- were prepared by using ^{13}C-enriched $NaHCO_3$.

The chemical shift of the mononuclear complex, 167.6 ± 0.1 ppm, has been determined from solutions where 100% of the total uranium is present as $UO_2(CO_3)_3^{4-}$. This can be compared with the value of 167.7 ppm obtained by Maya et al.[16] and with the value of 168.9 ± 0.2 ppm obtained by Strom et al.[17]

(5) Johansson, G. *Acta Chem. Scand.* **1971**, *25*, 2787.
(6) Åberg, M. *Acta Chem. Scand.* **1970**, *24*, 2901.
(7) Sandström, M.; Persson, I.; Ahrland, S. *Acta Chem. Scand., Sect. A* **1978**, *A32*, 607.
(8) Milberg, M. E. *J. Appl. Phys.* **1958**, *29*, 64.
(9) Johansson, G.; Sandström, M. *Chem. Scr.* **1973**, *4*, 195.
(10) Cromer, D. T.; Waber, J. T. *Acta Crystallogr.* **1965**, *18*, 104.
(11) Stewart, R. F.; Davidson, E. R.; Simpson, W. T. *J. Chem. Phys.* **1965**, *42*, 3175.
(12) Narten, A. H.; Levy, H. A. *J. Chem. Phys.* **1971**, *55*, 2263.
(13) Cromer, D. T. *Acta Crystallogr.* **1965**, *18*, 17.
(14) Cromer, D. T. *J. Chem. Phys.* **1969**, *50*, 4857.
(15) Compton, A. H.; Allison, S. K. "X-Rays in Theory and Experiment"; Van Nostrand: New York, 1935.
(16) Maya, L.; Begun, G. M. *J. Inorg. Nucl. Chem.* **1981**, *43*, 2827.
(17) Strom, E. T.; Woessner, D. E.; Smith, W. B. *J. Am. Chem. Soc.* **1981**, *103*, 1255.

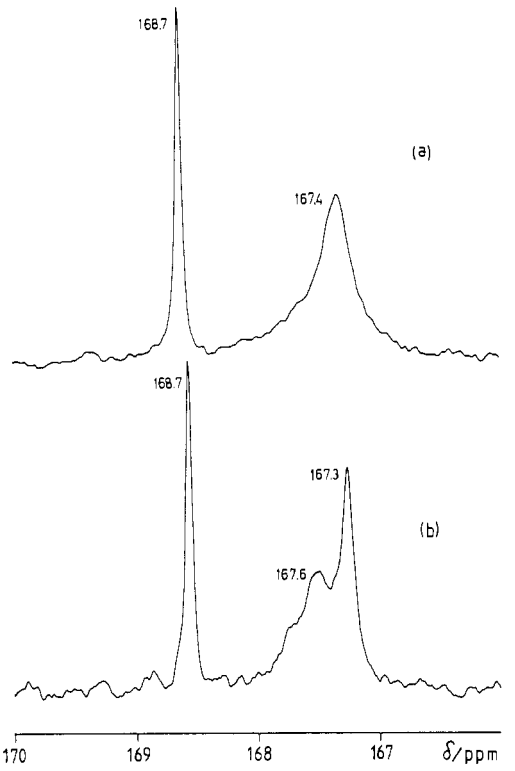

Figure 1. ^{13}C NMR spectra of a solution containing 50% of total uranium as $UO_2(CO_3)_3^{4-}$ and 50% as $(UO_2)_3(CO_3)_6^{6-}$ ($[UO_2^{2+}]_{total}$ = 98.3 mM; pH 5.7): (a) at ~22 °C; (b) at ~2 °C.

It is not possible to prepare a solution containing the trinuclear complex only. Some amount of mononuclear complex is always present. Spectra from these solutions contain in general two peaks (Figure 1a). The low-frequency peak is a composite and can be partially resolved by decreasing the temperature (Figure 1b) and/or by increasing the magnetic field.

^{13}C NMR spectra have been recorded for solutions with different ratios between the mononuclear and the trinuclear species (the solutions also contained varying amounts of excess hydrogen carbonate). By comparison of the composition of each solution with the values of the integrals of its ^{13}C spectra, the peaks at 168.7 and 167.3 ppm (see Figure 1b) can be assigned to two different, equally populated carbonate sites in the $(UO_2)_3(CO_3)_6^{6-}$ complex. These experimental results and their interpretation are in agreement with the data of Maya et al.[16] when account is taken of the poor resolution of the latter ones.

It seems probable that the low-frequency peak (167.3 ppm) originates from a type of carbonate ion similar to that present in the mononuclear complex, $UO_2(CO_3)_3^{4-}$ (167.6 ppm).

X-ray Diffraction. The $s[i(s)]$ values are shown in Figure 2. The radial distribution curves, $D(r)$, are given in Figure 3, and the $D(r) - 4\pi r^2\rho_0$ functions are shown in Figure 4. The radial distribution curves show peaks at 1.55, 2.5, 2.9, 4.25, and 4.9 Å but also at larger r values. The first peak at 1.55 Å corresponds to the unresolved C–O and N–O (solution C only) interactions within the planar CO_3^{2-} and NO_3^- groups, the Cl–O interactions (solutions B1 and B2) within the tetrahedral ClO_4^- ion, and the U–O interactions within the linear UO_2^{2+} group. The double peak at 2.5–2.9 Å corresponds to several interactions: U–O, U–C, and O–O interactions within the uranyl carbonate complexes; Na–O interactions within the $Na(H_2O)_6^+$ group; O–O interactions within the CO_3^{2-}, NO_3^-, and ClO_4^- groups and within the water structure. In the region 4.25–4.9 Å, longer U–O, U–C, O–O, and O–C interactions within the uranyl carbonate complexes as well as O–O interactions within the $Na(H_2O)_6^+$ group and the water structure

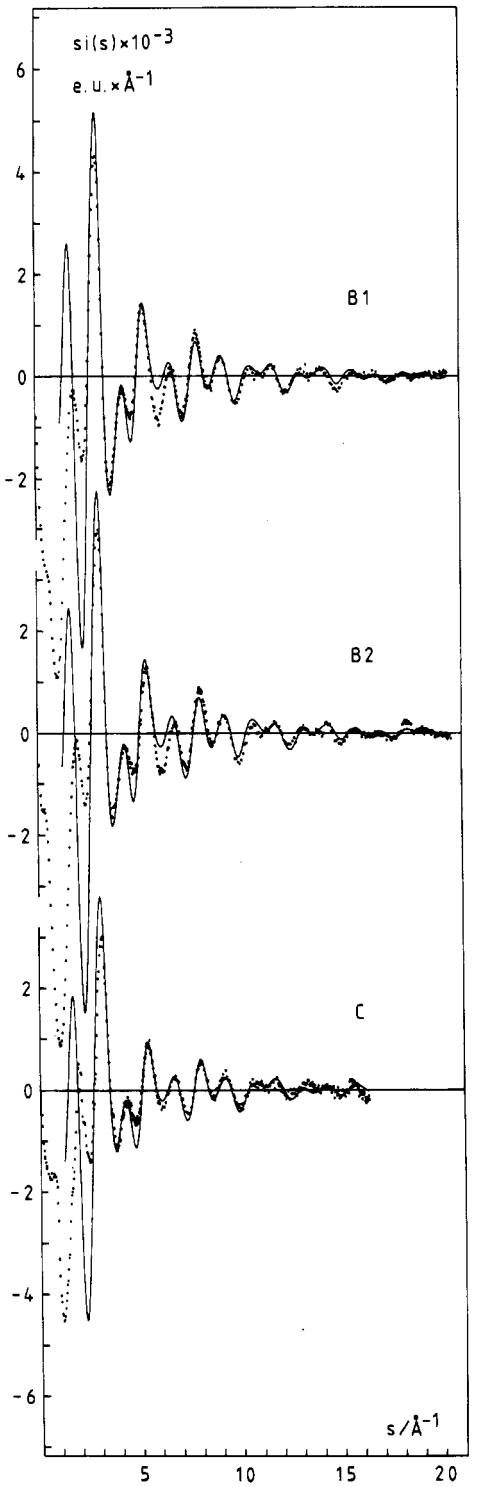

Figure 2. Reduced intensity functions $s[i(s)]$. The experimental values are given as dots. The full-drawn curves represent the intramolecular interactions calculated with use of the parameter values given in Table II.

are expected. The main contribution to the big 4.9-Å peak, however, originates from U–U interactions within the trinuclear $(UO_2)_3(CO_3)_6^{6-}$ complex.

The radial distribution curves show only one peak that can be attributed to U–U interactions. Therefore, the trinuclear complex is likely to be triangular.

A structural model for the carbonate solutions was constructed from tetrahedral ClO_4^- ions, tetrahedral $H_2O(H_2O)_4$ groups, octahedral $Na(H_2O)_6^+$ complexes, and $UO_2(CO_3)_3^{4-}$ and $(UO_2)_3(CO_3)_6^{6-}$ complexes. The studied solutions contained more than 80% of the total uranium as $(UO_2)_3(CO_3)_6^{6-}$

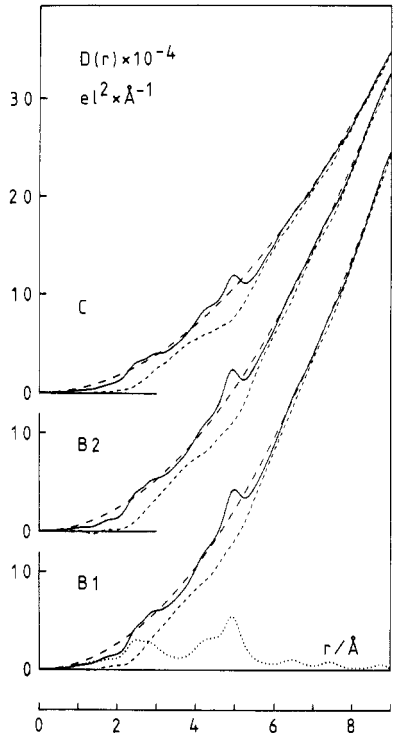

Figure 3. Radial distribution curves, $D(r)$. The experimental functions are shown as solid lines, and the functions calculated with use of the parameter values given in Table II are represented by dotted curves (only given for solution B1). The differences between them are marked by short dashes, and the functions $4\pi r^2\rho_0$ are indicated by long dashes.

(see Table I).

Three complete crystal structures have been reported for compounds containing the $UO_2(CO_3)_3^{4-}$ complex.[2-4] The uranyl group is equatorially surrounded by the three carbonate ions acting as bidentate ligands. In $(NH_4)_4[UO_2(CO_3)_3](s)$[2] and $K_4[UO_2(CO_3)_3](s)$,[3] the complex has a 2-fold rotation axis through the uranium atom and the C–O bond of one of the carbonate ions. In $CaNa_2[UO_2(CO_3)_3]\cdot xH_2O(s)$ ($x \simeq 5.6$),[4] there is a mirror plane through the uranyl group and one of the carbonate ions.

Table II. Parameter Values Used for the Calculation of Theoretical Curves

complex[a]	intramolecular dist r, Å	temp factors b, Å²
ClO_4^- tetrahedron	Cl-O 1.43	Cl-O 0.00072, O-O 0.00164
H_2O	O-H 1.0	O-H 0.004
$H_2O^I(H_2O^{II})_4$ tetrahedron	O^I-O^{II} 2.86	O^I-O^{II} 0.015, O^{II}-O^{II} 0.2
$Na(H_2O)_6^+$ octahedron	Na-O 2.41	Na-O 0.029, O-O 0.2
CO_3^{2-}	C-O 1.31	C-O 0.00085, O-O 0.0013

[a] For $UO_2(CO_3)_3^{4-}$ and $(UO_2)_3(CO_3)_6^{6-}$ values, see text.

For the interpretation of the scattering data, an idealized structure with D_{3h} symmetry for the $UO_2(CO_3)_3^{4-}$ complex has been assumed. The average values of the U–O coordination distances have been taken from recent references[3,4] (U–O(uranyl) = 1.80 Å, U–O(carbonate) = 2.43 Å).

The model for the trinuclear complex $(UO_2)_3(CO_3)_6^{6-}$ is based on the following experimental observations: (1) the formula of the complex is determined by the emf measurements,[1] (2) there are two sets of equivalent carbonates with three CO_3^{2-} in each set (cf. ^{13}C NMR section), and (3) there is only one U–U distance in the radial distribution curve.

By assuming an idealized D_{3h} symmetry, where the uranium coordination has a hexagonal-bipyramidal geometry as in

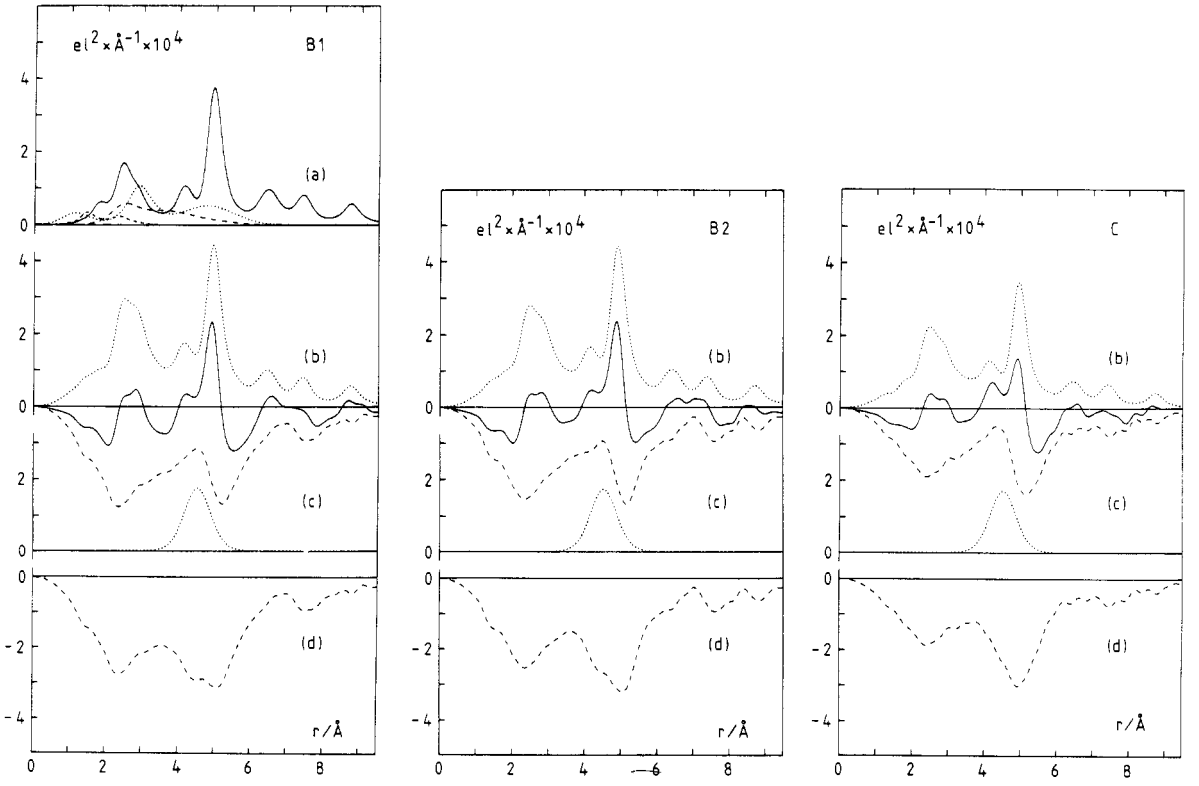

Figure 4. $D(r) - 4\pi r^2\rho_0$ functions and calculated peak shapes for the three carbonate solutions. In (a) peak shapes calculated separately for the complexes ClO_4^- (short dashes), $Na(H_2O)_6^+$ (long dashes), $H_2O(H_2O)_4$ (dots), and $UO_2(CO_3)_3^{4-}$ plus $(UO_2)_3(CO_3)_6^{6-}$ (solid line) are shown for solution B1. In (b) the full-drawn curve is the experimental function and the dotted curve represents the function calculated from the parameter values given in Table II. The difference between them is given as dashes. When the calculated peak shape for the second coordination sphere, which is shown in (c), is also subtracted, the difference curve in (d) is obtained.

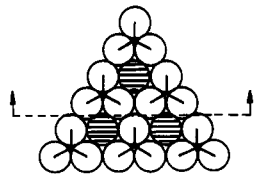

Figure 5. Suggested model for the trinuclear complex $(UO_2)_3(CO_3)_6^{6-}$ as derived from Figure 4 and from the structure of the mononuclear complex $UO_2(CO_3)_3^{4-}$ (indicated by dashes):[3,4] filled circles, uranyl groups; open circles, carbonate oxygens.

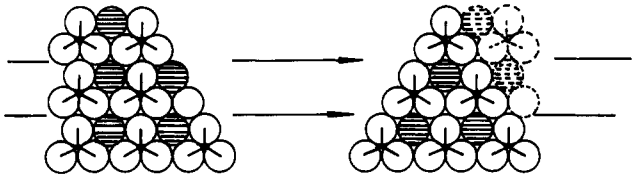

Figure 6. Relation between the structure of UO_2CO_3(s) (rutherfordine) (a) and the model suggested for $(UO_2)_3(CO_3)_6^{6-}$ (b). Atoms are represented in the same way as in Figure 5.

UO_2CO_3(s)[18] or $K_4[UO_2(CO_3)_3]$(s),[3] one can deduce a possible structure for the trinuclear complex (Figure 5). These structural features are also found in some solid actinoid carbonate structures, viz. $MNpO_2CO_3$ ($M = K^+$, Rb^+, Cs^+, NH_4^+).[19] The suggested structure is related to the structure of rutherfordine, UO_2CO_3(s) (Figure 6), by a translation as indicated in the figure.[20] The parameter values of the structural model for the solutions are given in Table II.

Approximate parameter values for the U–U interaction within the trinuclear complex could be estimated from the position and size of the peak in the radial distribution curve. More accurate values were obtained by least-squares refinement procedures using the high-angle part of the intensity curve to which the intramolecular interactions give predominant contributions.

The experimental reduced-intensity values, $i(s)$, were compared with calculated $\sum i_{pq}(s)$ values. For each pair interaction the distance, r_{pq}, the temperature factor, b_{pq}, and an occupancy factor, n_{pq}, were variables. A minimum was sought for the error-square sum $U = \sum w(s)[i(s) - \sum i_{pq}(s)]^2$. The weighting function $w(s) = (\cos\theta)/I^2(s)$ was chosen. With this weighting function, the contribution to U from each experimental point is inversely proportional to the square of its estimated standard deviation.

In least-squares refinements using experimental data for $s_{min} < s < 17$ Å^{-1}, where $s_{min} = 7$ and 9 Å^{-1}, the U–U distance and the temperature factor were varied. All other parameter values were kept constant. The average values obtained were $r_{U-U} = 4.942$ (3) Å and $b_{U-U} = 0.0042$ (2) Å^2 for solution B1 and $r_{U-U} = 4.951$ (4) Å and $b_{U-U} = 0.0046$ (3) Å^2 for solution B2.

Thereafter, a common temperature factor for the U–light atom interactions within the uranyl carbonate complexes was refined in least-squares refinements using experimental data for $s_{min} < s < 17$ Å^{-1}, where s_{min} was varied from 3 to 7 Å^{-1}. All other parameter values were kept constant. The average values obtained were $b = 0.0028$ (9) Å^2 for solution B1 and $b = 0.0037$ (12) Å^2 for solution B2.

With the refined parameter values and the values given in Table II, theoretical curves were calculated. The results are shown in Figures 2–4.

The suggested structural model for the trinuclear complex explains the high-angle part of the scattering curves ($s > 2.5$ Å^{-1}) fairly well. The main contributions in this region, besides U–U, come from U–O and U–C, and adjusting the parameter values for the light atoms might increase the agreement. But for such adjustments to be meaningful, data from a crystal structure determination are needed.

The difference curves in Figure 4b have a broad peak with a maximum at 4.5 Å, which probably cannot be attributed to light-atom interactions only. Part of it can be explained by assuming a second coordination sphere of water molecules around the uranyl carbonate complexes (Figure 4c). After subtraction of 12 U–OH_2 interactions at 4.5 Å ($b = 0.04$ Å^2), the new difference curves for $r < 5$ Å show peaks only in regions where light-atom interactions not included in the model are expected to occur (Figure 4d). This explanation is obviously not unambiguous, since e.g. contributions from ion pairing between the uranyl carbonate complexes and Na^+ ions would occur in the same region of the curves.

For solution C no least-squares refinements were performed due to the lower statistical accuracy of the scattering data and the uncertainty in the composition of the solution caused by the precipitation. The average parameter values for solutions B1 and B2 were used. As shown in Figure 2, the calculated $s[i(s)]$ values fit the experimental data equally well or even better for this solution than for the more accurately studied solutions. One explanation of this is that the contributions to the scattering data from the background of light-atom interactions within the remaining water structure and the medium anions are comparatively larger for the more dilute solutions (cf. Table I). Hence, adjustments of the parameter values of this background may increase the agreement between the experimental and calculated $s[i(s)]$ values in an intermediate s range for the more dilute solutions, while such adjustments have only a minor effect for the more concentrated solution. Systematic errors due to approximations and incompletenesses in the structural model for the solutions thus seem to be more important than statistical counting errors, errors in the corrections made in the treatment of the experimental scattering data, and errors in the compositions of the solutions.

Acknowledgments. We wish to thank Dr. Ulf Henriksson (Department of Physical Chemistry, The Royal Institute of Technology) for help in performing the NMR measurements. This work was supported by the Swedish Natural Science Research Council (NFR) and the Swedish Nuclear Fuel Supply Company through Project KBS.

Registry No. $(UO_2)_3(CO_3)_6^{6-}$, 75311-41-0.

Supplementary Material Available: A listing of primary experimental data in the form of $i(s)$ for the three solutions investigated by X-ray diffraction (7 pages). Ordering information is given on any current masthead page.

(18) (a) Christ, C. L.; Clark, J. R.; Evans, H. T., Jr. *Science* **1955**, *121*, 472. (b) Cromer, D. T.; Harper, P. E. *Acta Crystallogr.* **1955**, *8*, 847.
(19) Volkov, Yu. F.; Tomilin, S. V.; Visyashcheva, G. I.; Kapshukov, I. I. *Radiokhimiya*, **1979**, *21*, 668.
(20) One-dimensional X-ray diffraction data can be given a unique structural interpretation only in very simple systems. The structure proposed in this study is based on several different types of information as discussed in the X-ray diffraction section. Diffraction and NMR data do not exclude other models such as those with a slightly distorted trigonal symmetry and those with fluxional (on the NMR time scale) carbonate groups inclined to the U_3 plane. However, the latter model will give a planar time-averaged structure.